Integrating hydrologic modeling and satellite remote sensing to assess the performance of sprinkler irrigation

Zheng, Chaolei; Jia, Li; Menenti, Massimo; Hu, Guangcheng; Lu, Jing; Chen, Qiting; Jiang, Min; Mancini, Marco; Corbari, Chiara

Integrating hydrologic modeling and satellite remote sensing to assess the performance of sprinkler irrigation

Chaolei Zheng, Li Jia, Massimo Menenti, Guangcheng Hu, Jing Lu, Qiting Chen, Min Jiang, Marco Mancini & Chiara Corbari

Published online: 17 May 2024.

Submit your article to this journal

Article views: 103

View related articles

View Crossmark data

Taylor & Francis
Taylor & Francis Group

OPEN ACCESS

Check for updates

Integrating hydrologic modeling and satellite remote sensing to assess the performance of sprinkler irrigation

Chaolei Zheng [a], Li Jia [a,b], Massimo Menenti [a,c], Guangcheng Hu [a], Jing Lu [a], Qiting Chen[a], Min Jiang [a], Marco Mancini[d] and Chiara Corbari [d]

[a]Key Laboratory of Remote Sensing and Digital Earth, Aerospace Information Research Institute, Chinese Academy of Sciences, Beijing, China; [b]International Research Center of Big Data for Sustainable Development Goals, Beijing, China; [c]Faculty of Civil Engineering and Earth Sciences, Delft University of Technology, Delft, Netherlands; [d]Department of Civil and Environmental Engineering, Politecnico di Milano, Milano, Italy

ABSTRACT

Improving irrigation water management is a key concern for the agricultural sector, and it requires extensive and comprehensive tools that provide a complete knowledge of crop water use and requirements. This study presents a novel methodology to explicitly estimate daily gross and net crop water requirements, actual crop water use, and irrigation efficiency of center pivot irrigation systems, by mainly utilizing the Sentinel-2 MultiSpectral Instrument (MSI) imagery at the farm scale. ETMonitor model is adapted to estimate actual water use (as the sum of canopy transpiration and evaporation of water intercepted by canopy and evaporation from soil) at daily/10-m resolution, benefiting from the high-resolution Sentinel-2 data and thus to assess the irrigation efficiency at the farm scale. The gross irrigation water requirement is estimated from the net crop water requirement and the water loss, including the water droplet evaporation directly into the air during application before droplets fall on the canopy and canopy interception loss. The method was applied to a pilot farmland with two major crops (wheat and potato) in the Inner Mongolia Autonomous Region of China, where modern equipment and appropriate irrigation methods are deployed for efficient water use. The estimated actual crop water use showed good agreement with the ground observations, e.g. the determination coefficients range from 0.67 to 0.81 and root mean square errors range from 0.56 mm/day to 1.24 mm/day for wheat and potato when comparing the estimated evapo-transpiration with the measurement by the eddy covariance system. It also showed that the losses of total irrigated volume were 25.4% for wheat and 23.7% for potato, respectively, and found that the water allocation was insufficient to meet the water requirement in this irrigated area. This suggests that the amount of water applied was insufficient to meet the crop water requirement and the inherent water losses in the center pivot irrigation system, which imply the necessity to improve the irrigation practice to use the water more efficiently.

1. Introduction

Irrigated agriculture is the largest water user in the world, and irrigation water use accounts for approximately 70% of global freshwater withdrawals (Carpenter, Stanley, and Vander Zanden 2011). Climate change and increasing human water demand, combined with traditional wasteful irrigation practices, are exacerbating water use conflicts, even in traditionally water-rich countries. Saving a small amount of water in agriculture can significantly reduce water scarcity pressure in other sectors. Irrigation water management with properly considering the crop water use and requirements is important in addressing regional to national water security issues, especially in developing countries (Lankford 2023; Liu et al. 2024).

A first and obvious need is the ability to assess, monitor, and understand water use. The evaluation of irrigation water use performance has evolved significantly over the last few decades, and it essentially requires some primary data, such as irrigated areas, irrigation types, crop irrigation water requirements, and actual evapotranspiration. For small irrigation schemes, the required local information can be collected directly from farmers. However, the field survey is time-consuming, labor-intensive, and can only be conducted in a limited number of locations. For large systems, experience shows how difficult it is to collect accurate data on actual water use by traditional methods (Levidow et al. 2014; Menenti 2000). In this context, the effectiveness or adequacy of any irrigation system depends largely on its efficiency in terms of water use and loss, which are influenced by irrigation technology, drainage infrastructure, water management, soil, and topography (Evans and Sadler 2008; Renault 1999). Satellite remote sensing

---

CONTACT Li Jia ✉ jiali@aircas.ac.cn

datasets can support irrigation management (Bastiaanssen and Bos 1999; Bwambale et al. 2022; D'Urso 2010; Dari et al. 2023; Knipper et al. 2019), due to the frequent revisit time, cost-effectiveness, and high spatial resolution which are very helpful for heterogeneous irrigated lands. Numerical hydrological models are also widely used to simulate crop water requirements and water uses to optimize irrigation practices (Corbari et al. 2019). Hydrological models could be coupled with either ground observations or remote sensing to simulate vegetation indices, evapotranspiration, soil moisture, etc. Fully integrated uses of satellite data, ground-based hydro-meteorological data, and numerical modeling are needed to support water resources management of agricultural farms as well as large un-gauged agricultural areas.

Irrigation systems play an important role in agriculture. Center pivot irrigation system (CPIS) is widely used all over the world, especially in those regions where groundwater is the main water resource, because it is labor-saving and water-consuming efficient. In the case of irrigation water use, water loss occurs at several levels depending on the type of irrigation being practiced. For example, infiltration through the canal bed (Gray and Norum 1967; Rivett et al. 2016; Sayari, Mahdavi-Meymand, and Zounemat-Kermani 2021), evaporation from the open water surface (Penman 1948; Uddin and Murphy 2020), intercepted water (Gash, Lloyd, and Lachaud 1995; Herbst et al. 2008; Lin, Sadeghi, and Van Stan 2020; Lloyd et al. 1988), droplet evaporation during sprinkling (Molle et al. 2012; Thompson, Gilley, and Norman 1993; Yazar 1984). In sprinkler irrigation, the water flow emitted from the sprinkler heads (nozzles) forms water jets (ribbons) that break up into droplets due to surface tension and aerodynamic drag forces as they travel from the nozzle to the soil surface. During the flight, a fraction of the water droplets evaporates (called droplet evaporation). Increasing the operating pressure of the sprinkler head decreases the resulting droplet diameters and increases the evaporation losses due to the increased water–air interface area. The remaining portion of the water is partitioned between canopy interception and direct throughfall to the soil. The intercepted water evaporates in response to the atmospheric demand, but not crop water requirements, and is referred to as interception loss (Tolk et al. 1995; van Dijk et al. 2015). These processes could not be captured by satellite remote sensing, but they could be described in the hydrological model. This also highlights the need to integrate hydrological modeling with satellite imagery to assess crop water use and irrigation performance under sprinkler irrigation.

Studies have been carried out in the past, but rarely all the components have been integrated to understand the gross irrigation water requirements for optimal crop growth, actual water use and water loss at different stages of irrigation application using high-resolution remote sensing data. In this paper, we propose a new approach that integrates the advantages of hydrological modeling and high-resolution multi-spectral remote sensing data, mainly from Sentinel-2, to estimate the water requirements at field scale and to estimate the amount of water used at different levels relative to the requirements within an irrigation scheme. These estimates are incorporated into various indicators to evaluate the irrigation performance of the CPIS irrigation system.

2. Methodology

To evaluate the irrigation performance, a novel method is proposed to explicitly estimate different variables related to water use, water loss, and water requirement, using hydrological modeling and multi-spectral remote sensing data (e.g. Sentinel-2). It mainly consists of three main parts: 1) estimation of the field-scale actual consumptive water use, as the sum of the canopy transpiration (E_c), soil surface evaporation (E_s), evaporation of canopy intercepted water (E_i), and droplet evaporation directly from the air during irrigation application (E_A); 2) estimation of the irrigation water requirement, including gross irrigation water requirement ($GIWR$) and net irrigation water requirement ($NIWR$), taking into account the water losses within the irrigation system; 3) estimation of the irrigation performance indicators (IPs), which were finally used to evaluate the performance of the irrigation system. The overview of the approach is illustrated in Figure 1. Details on the utilized data are described in Section 3.2.

The proposed methods have several advantages, including 1) rather than estimating the total water use directly by a combination method, our method provides explicitly the components of consumed water amount, i.e. droplet evaporation, intercepted water evaporation, transpiration, soil evaporation, which enable to separate the benefit and non-benefit water flow that are very important to guide the further water-saving technologies development; 2) by integrating hydrological modeling with the high-resolution satellite remote-sensing data, this method can provide both temporal and spatial variations of the water use with very high resolution, which are critical for the stakeholders to adapt their management practices more precisely; 3) a new irrigation indicator was combined with existing indicators in the method to provide a comprehensive evaluation of the irrigation water management, which takes into account the inherent water losses in the specific irrigation technique.
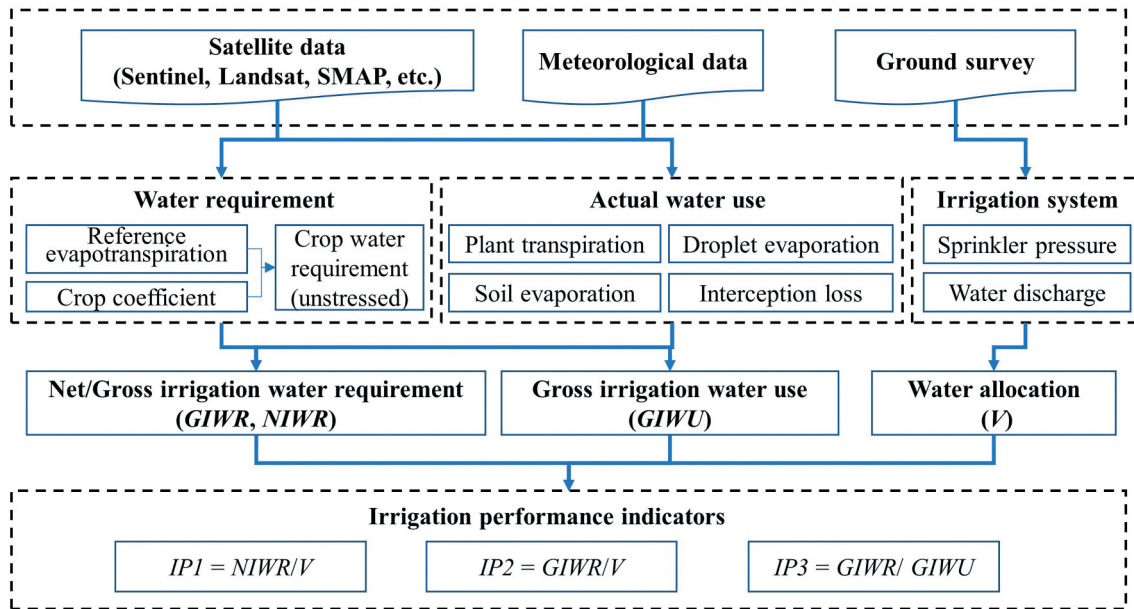
Figure 1. Overview of the methodology to evaluate the irrigation performance under sprinkler irrigation system in this study.

2.1. Estimation of actual gross irrigation water use under the sprinkler irrigation systems

Water use under sprinkler irrigation is affected by losses at several processes (e.g. water droplet vaporized in the air, water intercepted by the crop canopy, water evaporated from the top soil layer) until the water reaches the crop root zone to be absorbed and utilized by the crop. These processes occurred at different temporal and spatial scales, e.g. the water droplet vaporized in the air occurs during the water "flight" from the nozzle to crop or soil while sprinkling, and the water intercepted by the crop canopy partly evaporated to the air after the irrigation events. It is necessary to quantify these losses at different hierarchical scales to properly account for each process (Pani et al. 2020). To estimate the irrigation water use, the consumptive water use (CWU, in mm) is first estimated as the sum of actual evapotranspiration (ET_a) from the surface (including the crop canopy and soil surface) and droplet evaporation during the sprinkling of the applied irrigation system. The CWU under the sprinkler irrigation equals to:

$$CWU = E_c + E_s + E_i + E_A \qquad (1)$$

where E_c (mm) is the crop transpiration, E_s (mm) is the soil evaporation, E_i (mm) is evaporation of canopy intercepted water (also called canopy interception loss, zero on non-irrigation and non-rainfall days), and E_A (mm) is the droplet evaporation during the "flight" from the nozzle to crop or soil while sprinkling (zero on non-irrigation days). The ET_a ($ET_a = E_c + E_s + E_i$) and its components from the crops canopy and soil surface are estimated using ETMonitor model (Hu and Jia 2015; Zheng, Jia, and Hu 2022), which is described

briefly in Section 2.1.1. And section 2.1.2 introduces the method to estimate E_A.

All the above components of water use were estimated for each pixel at daily/10-m resolution in this study. The total CWU in a growing season for each field (field size is much larger than 10 m) that contains one crop under sprinkler irrigation can be written as:

$$CWU_k = \sum_{j=0}^{J} \frac{\sum_{i=1}^{n}(CWU_{ij})}{n} \qquad (2)$$

where j is an individual day in a growing season with total J days; i is the smallest unit area in the study area, i.e. a 10-m pixel in Sentinel-2 image; and n is the total number of pixels in a single field with the same crop. The gross irrigation water use ($GIWU$) can be expressed as the area-weight average of CWU in each field cultivated by a specific crop, as:

$$GIWU = \frac{\sum_{1}^{K}(CWU_k \times af_k)}{\sum_{1}^{K} af_k} - P_{eff} \qquad (3)$$

where k is an individual field containing a specific crop with total K number of fields in the irrigation scheme, af_k is the area of each field, P_{eff} is the effective precipitation calculated according to Kuo et al. (2006):

$$P_{eff} = P_{tot} \frac{125 - 0.2P_{tot}}{125} \qquad (4)$$

where P_{tot} is the total rainfall for the whole growing season (mm).

2.1.1. Estimation of actual ET components using ETMonitor model

The actual land surface ET components, including E_c, E_s, and E_i in Equation (1), are estimated at daily scale using ETMonitor model, which is a hybrid evapotranspiration estimation model that combines theories of energy balance, plant physiology, and water balance processes (Hu and Jia 2015; Zheng, Jia, and Hu 2022). The model is forced by a variety of biophysical parameters and surface soil water status, which are derived from multi-source remote sensing data (from optical to microwave sensors). The ETMonitor model was presented and applied for ET estimation in the arid and semi-arid land (Hu and Jia 2015), in humid regions (Zheng et al. 2019) and global ET estimation (Jia et al. 2018; Zheng et al. 2016, 2022), and was also used for various applications (Bennour et al. 2022; Buri et al. 2024; Chen et al. 2019, 2023; Du et al. 2022; Jia et al. 2021; Menenti et al. 2021).

The ETMonitor model consists of several modules to simulate ET components, including plant transpiration, soil evaporation, vegetation canopy interception loss, water body evaporation, and snow/ice sublimation. In ETMonitor, E_c and E_s are estimated using the Shuttleworth – Wallace two-source scheme (Shuttleworth and Wallace 1985), combined with a Jarvis-type method for estimating canopy resistance to transpiration, where the minimum canopy resistance is regulated by soil moisture and other environmental variables (Jarvis 1976; Steward 1988). E_i is estimated using a revised Gash model (Gash, Lloyd, and Lachaud 1995; Zheng and Jia 2020), which is a rainfall event-based model that has been successfully applied on a daily basis, assuming one storm per rainy day. More details on the ETMonitor model and the implementations could be found in previous studies (Hu and Jia 2015; Zheng and Jia 2020; Zheng, Jia, and Hu 2022). The main driving data of ETMonitor include the leaf area index (LAI), fraction of vegetation cover (FVC), surface albedo, soil moisture, which could be obtained from satellite remote sensing datasets, and meteorological forcing data either from ground observations or atmospheric reanalysis data.

2.1.2. Estimation of droplet evaporation during sprinkling

A considerable amount of water droplets evaporates directly in the air (E_A in Equation(1)) during sprinkling irrigation without ever reaching the crop canopy or soil surface. E_A is affected by several factors such as wind speed, sprinkler height (when the crop is shorter during the growing season), longer drop trajectory and increased wind exposure (Playán et al. 2005; Stambouli et al. 2013). Quantifying this amount is complicated and challenging but is very necessary to address the water balance in sprinkler irrigation.

Droplet evaporation can be parameterized using a semi-empirical equation proposed by Yazar (1984):

$$E_A = 0.003 \exp{(0.20u)(e_s - e_a)^{0.59}(T_a^{0.23})(P_S^{0.76})(D_{IS})}$$

$$(5)$$

where u is the wind speed (km/h), e_s and e_a are the saturated and actual vapor pressure (mb), T_a is the air temperature (°C), P_S is the sprinkler operating pressure (kPa), and D_{IS} is the amount of water discharged from the sprinkler (mm). In this study, u, e_s, e_a, and T_a are obtained from local weather observations, P_S and D_{IS} are calculated considering the dynamic of CPIS (Martin, Kincaid, and Lyle 2007; Yazar 1984).

Specific to the dynamic of CPIS irrigation system, the sprinkler heads are adjusted in such a way that the water pressure of each nozzle increases linearly with the distance from the center to the outer boundary during discharge to avoid excessive discharge from nozzles near the center. Therefore, P_S and D_{IS} are calculated in a dynamic approach following previous studies (Martin, Kincaid, and Lyle 2007), which can give the spatial distribution of D_{IS} for each pixel of satellite imagery where a sprinkler is operating at pressure P_S. The volumetric discharge per sprinkler was estimated to vary between 580 and 81,000 liters per irrigation using the field information on the maximum capacity of the pump (22.2 lt./s). The discharge of a single sprinkler varied as designed in response to P_S, which varied between 0.1 and 131 kPa from the center to the outer lateral end. Therefore, we estimated that E_A varied between 0.12 and 2.6 mm per irrigation (72 h) under reference condition (wind speed of 3.9 km/h VPD 1.4 mb, and air temperature 21°C), depending on the operating pressure of each sprinkler nozzle. E_A increased logarithmically from the center to the outer lateral end, due to the increase in the area wetted by each sprinkler along the lateral.

2.2. Estimation of irrigation water requirement

The estimation of irrigation water requirements mainly involved three key variables: *GIWR*, *NIWR*, and water losses within the irrigation system. *GIWR* is the sum of *NIWR* and water losses within an irrigation system, which is given below,

$$GIWR = NIWR + losses \qquad (6)$$

The estimate of on-farm water *losses* in Equation (6) is for reference conditions, i.e. it is taken as the estimated long-term average of losses due to droplet evaporation and interception loss over the entire growing season. The *NIWR* for the growing season is the average irrigation water requirement (*IWR*) over the *K* fields in the irrigation system, and the *IWR* is the difference between the crop water requirement (*CWR*, maximum crop

Table 1. Irrigation performance indicators used in this study.

Irrigation performance	Simplified Formula	Remarks	Reference
IP1	NIWR/V	based on potential ET and volume of water allocation	Menenti (2000)
IP2	GIWR/V	Based on actual ET and volume of water allocation	Menenti et al. (1989)
IP3	GIWR/GIWU	Proposed in our previous study	Pani et al. (2020)

evapotranspiration of a given crop under unstressed conditions) and the effective mean precipitation:

$$IWR = ET_c - P_{eff} \qquad (7)$$

where ET_C is the "potential" or maximum evapotranspiration for each crop, and it is estimated as:

$$ETc = ET_0 k_c \qquad (8)$$

where ET_0 is the reference evapotranspiration calculated according to FAO-56 (Allen et al. 1998), and k_c is crop coefficient estimated following Calera et al. (2017) according to its relationship with Normalized Difference Vegetation Index (NDVI) as:

$$k_c = a \times NDVI + b \qquad (9)$$

where a and b are the empirical parameters that vary with the crop types (in this study, a = 1.64 and b =-0.12 for wheat, a = 1.36 and b = 0.2 for potato).

2.3. Irrigation system performance indicators

In this study, we have used two well-defined Performance Indicators (*IPs*) (Menenti 2000; Menenti et al. 1989), as well as a new performance indicator considering both *GIWR* and *GIWU* (Pani et al. 2020). These *IPs* are listed in Table 1. *IP1* provides information on the adequacy of water allocations to meet water requirements for optimal crop growth. *IP2* provides information on the overall efficiency of the system in conveying, distributing, and applying irrigation water. *IP3* provides information on anomalies in water allocation and application that result in deviations of actual water use from water requirements, taking also into account the water losses inherent in the specific irrigation technique (in this study, sprinkling).

In all the *IPs* mentioned above (Table 1), the water allocated by irrigation managers or the actual use of water is used as the denominator to assess whether crop water requirements are met by the water provided, following the definitions proposed by Menenti et al. (1989). Values of *IP* greater than one indicate insufficient water supply, while values less than one indicate that applied/used irrigation water exceeds water requirements (Menenti 2000). A range of ± 0.15 (15%) from unity is considered efficient and acceptable in the current study.

3. Study area and data

3.1. Study area

We carried out this study in the irrigated agricultural area (Figure 2) located in the Zhenglan county in the north-central Inner Mongolia Autonomous Region of China. This study area is located between 41°59' N – 42°01' N latitude and 115°55' E – 115°57' E longitude. The local farmland is well equipped with modern irrigation infrastructure and contributes to a large production of wheat, oats, and a variety of vegetables. The most widely used irrigation method in this region is CPIS. The growing season is limited to the summer (April–September) due to the sub-freezing temperatures prevailing during the winter season. The experimental site shown in Figure 2 is covered by six CPIS fields. Each CPIS covers approximately 384,845 m² (38.5 ha), where wheat and potato are grown in alternate seasons. The source of irrigation is groundwater pumped directly from the center of each field. A flux tower (marked in red in Figure 2), with an eddy covariance system and an automatic weather station mounted in a tripod, is installed at the border of a field to gather water and heat flux and meteorological variables. As the major water source for irrigation comes from groundwater, the local water management faces great challenges. To our knowledge, this is the first comprehensive evaluation of the irrigation performance of the CPIS irrigation system based on high-resolution remote sensing data in the study region.

3.2. Data

3.2.1. Satellite data

Satellite remote sensing retrieval is innovative in this research to provide spatiotemporal information on the agricultural fields. To meet this need, multiple satellite data are used to estimate the variables and parameters described above. The data used in this study are listed in Table 2., These data could also be replaced by datasets from other satellite with similar sensors and configuration, when more advance satellite datasets are available

Biophysical variables and albedo retrieved from Sentinel 2 MSI and Landsat 8 OLI observations. A total of 19 cloud-free images are collected from Sentinel-2A & 2B Level-2A (L2A) MultiSpectral Instrument (MSI) radiometric data (with spatial resolution between 10 m and 60 m) during the growing season of 2019 (27th April–4th October). The Level-2 MSI data are geometrically and atmospherically corrected (Schläpfer et al. 1998) for top-
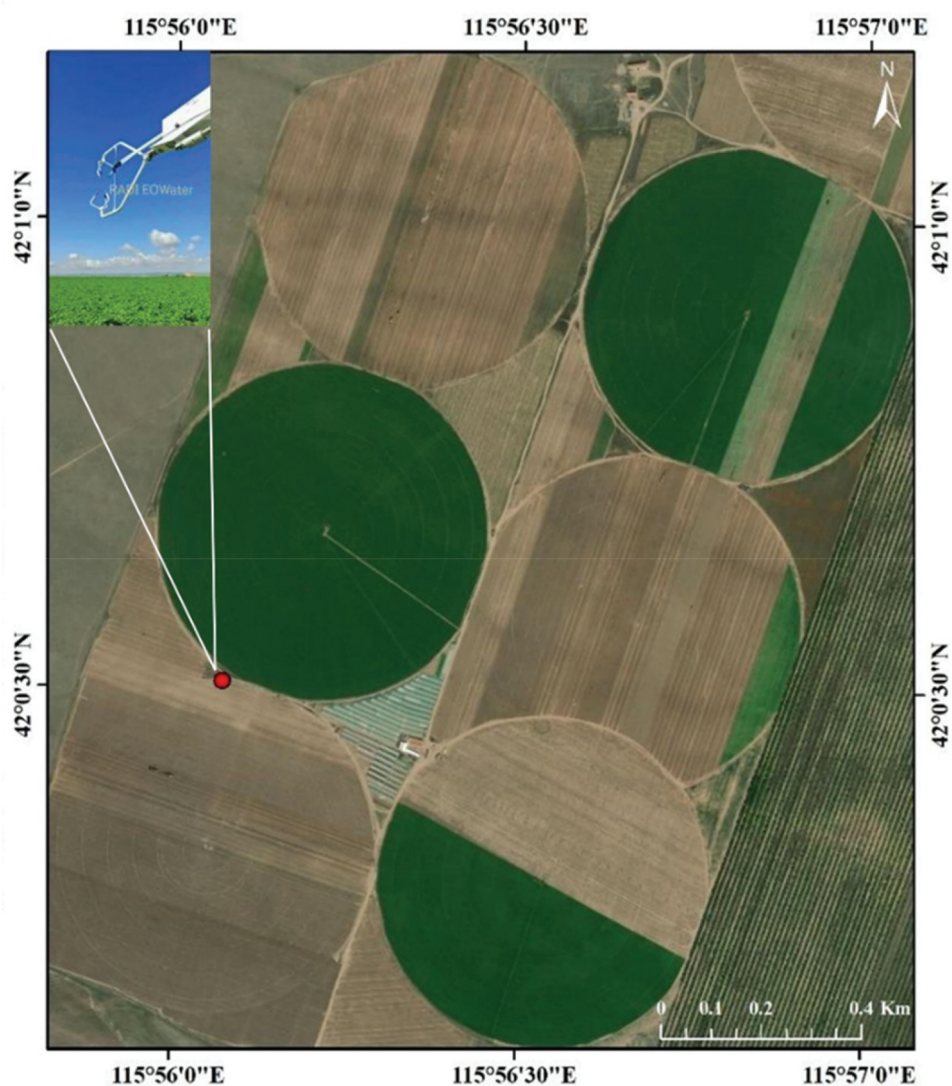
Figure 2. Study area in Inner Mongolia Autonomous Region in China with the location of the flux tower. The red dot indicates the location of the installed flux tower.

Table 2. List of datasets used in this study.

Dataset	Variables	Spatial Resolution	Temporal Resolution	Links
Sentinal-2 A&B MSI	Surface reflectance	10m	5 days	https://scihub.copernicus.eu/
Landsat-8 OLI	Surface reflectance	30m	16 days	https://search.earthdata.nasa.gov/
SMAP soil moisture	Surface/root-zone soil moisture	9km	3 hours	https://search.earthdata.nasa.gov/
CHIRPS 2.0	Rainfall	5km	Daily	https://chg-ftpout.geog.ucsb.edu
Meteorological Data	air temperature; dewpoint temperature; downward solar/ thermal radiation; wind speed; air pressure	25km	Hourly	https://cds.climate.copernicus.eu/
Soil parameter	Saturated/residual soil moisture	1km	–	http://globalchange.bnu.edu.cn/

of-canopy (TOC) reflectance and available to users from the European Space Agency (ESA) server (https://scihub.copernicus.eu/). Considering the unavoidable gaps due to cloud cover and satellite revisits may not allow to capture the full temporal evolution of crop water requirements based on single data source (Akdim et al. 2014; Mandanici and Bitelli 2016; Zhou et al. 2016), Landsat-8 Operational Land Imager (OLI) Collection-1 Level-2 Land Surface Reflectance products are also collected from the Earth Resources Observation and Science (EROS) Center, which provides atmospherically corrected (Vermote and Kotchenova 2008) data on-demand, as multispectral images at the

spatial resolution of 30-m (15-m for panchromatic) and a revisit time of 16 days (Roy et al. 2014). It was also found that there is a high correlation (with correlation coefficient of 0.98–0.99) between bands of MSI & OLI in terms of radiometric properties (Table 3). The combination of Sentinel 2 MSI and Landsat 8 OLI increases the temporal resolution for time-series analysis significantly (Tariq et al. 2023).

Different biophysical variables, i.e. NDVI, FVC, and LAI, were retrieved at high resolution (10 m) based on the multispectral bands from Sentinel 2 MSI and Landsat 8 OLI combination. To achieve this, the band 4 (red) and band 8A (vegetation red edge) of MSI and corresponding band 4 (red) and band 5 (NIR) of OLI are resampled from 20 m and 30 m to 10 m resolution, to match with the 10 m band 4 of MSI. The same approach was adopted to compute the albedo (Liang et al. 2003) using bands (2, 4, 8A, 11, 12) of MSI and bands (2, 4, 5, 6, 7) of OLI. Linear interpolation was applied to the available cloud-free images to create a daily time-series of all variables to capture the changes in crop growth.

The remote sensing retrievals of FVC and LAI were used to estimate the fraction of net radiation (R_n) absorbed by the canopy and soil in the ETMonitor to estimate E_c and E_s following Zheng et al. (2022). Albedo (α) is used to estimate R_n in the ETMonitor. FVC and LAI are also used to estimate vegetation storage of a canopy to determine the amount of intercepted water loss (E_i). NDVI is used to calculate and map the crop coefficient (k_c) for wheat and potato fields at different growth stages.

Soil Moisture from SMAP. Soil Moisture is also a key input variable for ET estimation using ETMonitor model. We have used Level-4 soil moisture data of the Soil Moisture Active and Passive (SMAP) L-band radar and radiometer observations. SMAP L4 Global 3 hourly 9 km EASE-Grid Surface and Root Zone Soil Moisture Analysis Update (SPL4SMAU) Version 4 (Reichle et al. 2018) are documented by NASA Earthdata (https://earthdata.nasa.gov). The objective of capturing the daily variation in the root-zone soil moisture content (m^3/m^3) was met by averaging the 3-hourly data to estimate the mean daily root-zone soil moisture.

Table 3. Correlation between the multispectral bands of Sentinel-2 MSI and Landsat 8 OLI.

Bands		
MSI Band	OLI band	Pearson Correlation Coefficient
2	2	0.9937
3	3	0.9944
4	4	0.9952
8	5	0.9853
8A	5	0.9967
11	6	0.9981
12	7	0.9984

3.2.2. Meteorological observations from ERA5 reanalysis data

Hourly radiation flux and meteorological observations were obtained from the European Centre for Medium-Range Weather Forecasts (ECMWF) ERA5 reanalysis data at a spatial resolution of 0.25 degree (https://cds.climate.copernicus.eu/). Hourly data were averaged to obtain daily mean values. Given the limited spatial variability of atmospheric variables (compared to land surface properties), spatial interpolation (Srivastava et al. 2019) was applied using inverse distance weighted (IDW) interpolation and resampled to 10 m to match the remotely sensed spatial data discussed above.

3.2.3. In-situ ground observation

In-situ information is a key input for optimizing on-farm water use. This was accomplished by conducting a thorough survey of the agricultural fields, collecting information on local farmers' irrigation practices, irrigation system specifications, and field experiments to measure the water discharge and interception losses in different crops.

Sprinkler specifications and local irrigation practices. The study area is covered by six large central pivot sprinkler systems of approximately 33.35 ha each and is irrigated with groundwater. Groundwater is pumped to the six systems by a total of 3 large (30 kW/h) and 11 small (8 kW/h) hydraulic pumps in total. Each CPIS, operating at 100% of the pump capacity, can pump water at a rate of 100 tons/h ~100 m^3/h. According to local farmers, this maximum capacity is rarely used in order to maintain the irrigation system and to avoid run-off. The farmers irrigate each field based on their experience of the average water requirements of each crop and the local weather conditions. They regulate the amount of water entering the system (Table 4) depending on the crop type and its growth stage to maintain optimal growth.

Ground measurements for model validation. Field experiments were carried out during the early and mid-growing seasons to measure several variables, namely crop type, crop height, volumetric water output from the sprinkler head, amount of water reaching the top of the canopy, and amount of water intercepted by the potato and wheat plants (Figure 3). The volumetric discharge, amount of water reaching the top of canopy and interception loss were measured on 13th and 14th of July, 2019. The mean FVC on 13th and 14th July, 2019 was 0.74 and 0.69 with LAI of 2.75 and 2.38 for wheat and potato, respectively. The crop heights were 0.9 m (wheat) and 0.79 m (potato). To capture the variation in the volumetric discharge from sprinkler along the lateral as well as the amount reaching the top and bottom of the canopy, the Differential Measurement Technique (DMT) was applied using a tipping bucket rain gauge at 30 different locations including both crops at varying distances from the center of the field (Figure 4). The difference between

Table 4. Irrigation schedule applied by farmers during growing season for different crops in the study area in 2019.

Crop Type	Period	Irrigation frequency	Number of irrigation events	Percentage of pump capacity (%)	Rate of in-flow (m^3/h)
Wheat	27th April-31th May	once in 10–15 days	3	50	50
	1st June-15th July	irrigate for 5 days, stop for 2 days	14	80	80
	16th – 31th July	once every 5 days	2	80	80
	1st Aug – Harvest	once every 5 days	5	30	30
Potato	5th May-22th May	no irrigation	0	0	0
	22th May – 30th June	once in 12–15 days	3	50	50
	1st July – 10th Aug	continuous irrigation	14	80	80
	11th Aug – Harvest	once every 5 days	7	30	30

Figure 3. Crop stages during field inspection and measurement in 2019 in the study area.
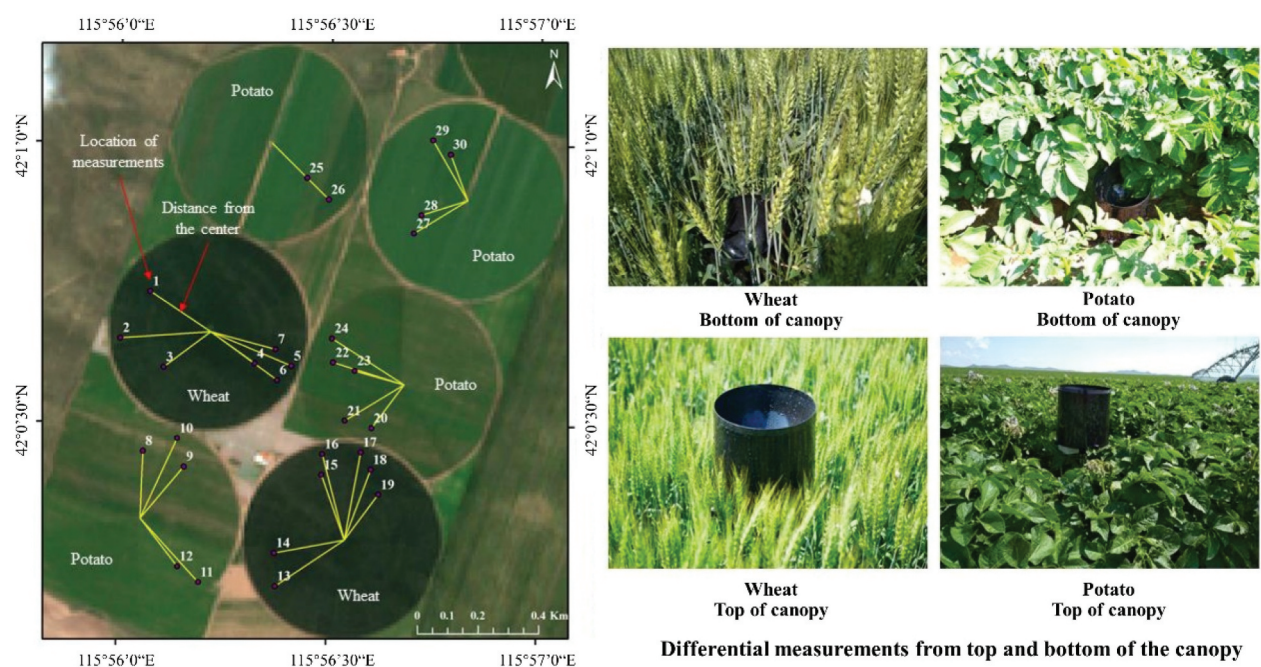

Figure 4. Locations of the tipping bucket rain gauge during the field experiment and the distance from the center during the growing season of 2019 in the study area.

the discharge from sprinkler head and the water reaching the top of the canopy was considered the amount of droplet evaporated directly, while the difference in the amount of water between the top and bottom of the canopy gave the amount of water intercepted by the canopy.

Flux tower observation for ET validation. The RS-based ET estimates were validated using ET measurements by the eddy covariance system in the flux tower (Zheng et al. 2021). The flux observations at 30-minute interval were aggregated to daily scale after a thorough quality check of the data and elimination of the outliers. The instrument was able to measure the ET of both potato and wheat as it was installed at the edge of both fields adjacent to each other. The measurements were intelligently assigned to the two crops based on the wind direction to identify the measurement source area.

4. Results and discussion

4.1. Validation of the estimated water use components

To validate the water use, the daily estimates of actual ET_a from ETMonitor were compared with in-situ measurements from the eddy covariance system. Unlike ETMonitor, which provides separate estimates of E_c, E_s and E_i, the eddy covariance system measures the sum of E_c and E_s during non-rainy and non-irrigated day. During the rainfall or irrigation days, the eddy covariance system theoretically measures the sum of E_c, E_s and E_i. Therefore, the ETMonitor estimates of daily E_c and E_s on non-irrigation days were summed and compared with the eddy-covariance measurements of ET_a. The ETMonitor estimates at daily scale were in close agreement with the measurements for both potato and wheat (Figure 5), with determination coefficients (R^2) = 0.81 and Root Mean Square Errors ($RMSE$) = 0.56 mm/day for potato and R^2 = 0.67 and $RMSE$ = 1.24 mm/day for wheat. The

accuracy of estimated ET is comparable to previous study which showed that the ETMonitor-estimated daily ET at 1-km resolution has an $RMSE$ and correlation coefficient (R) of 0.93 mm/d and 0.75 when comparing with observations from 251 flux towers around the world, with more than 80% of the sites having $RMSE$ smaller than 1.2 mm/day (Zheng, Jia, and Hu 2022). The shorter distance between the location of the eddy covariance system and the potato field, i.e. 1.5 m for potato and 6 m for wheat, could possibly explain the better agreement and the higher correlation for the potato than for the wheat field. Meanwhile, the uncertainty of the observed data and assignment (described in Section 3.2) should be noticed. For simplification, we assigned the flux tower observed data to either potato or wheat according to the wind direction, which is reasonable because the direction of the source areas contributing to the measured fluxes at flux tower sites (i.e. flux footprint) varies largely depending on wind direction. A more comprehensive method, e.g. two-dimensional parameterization for flux footprint prediction model to identify both the direction and extent of the flux footprint (Kljun et al. 2015), can be helpful for ET validation (Chu et al. 2021). The estimated ET_a varied between 3.9 and 8.1 mm/day for potato and between 0.19 and 8.1 mm/day for wheat with most values below 4.2 mm/day. These ET_a values are within the reasonable range of the previously reported values (Chen et al. 2023; Liu et al. 2013). The lower ET value observed for wheat in Figure 5 may be attributed to the fact that only a few flux data during the peak growing period were assigned to the wheat field. During the peak growing stage with high ET values, the dominant wind direction is southward, resulting in the observed flux being mainly from the potato field.

The estimated E_i was validated using the DMT observations to measure the irrigation water reaching the top and bottom of the canopy as described in Section 3.2.3. A comparison of measured and estimated E_i shows a better agreement for wheat

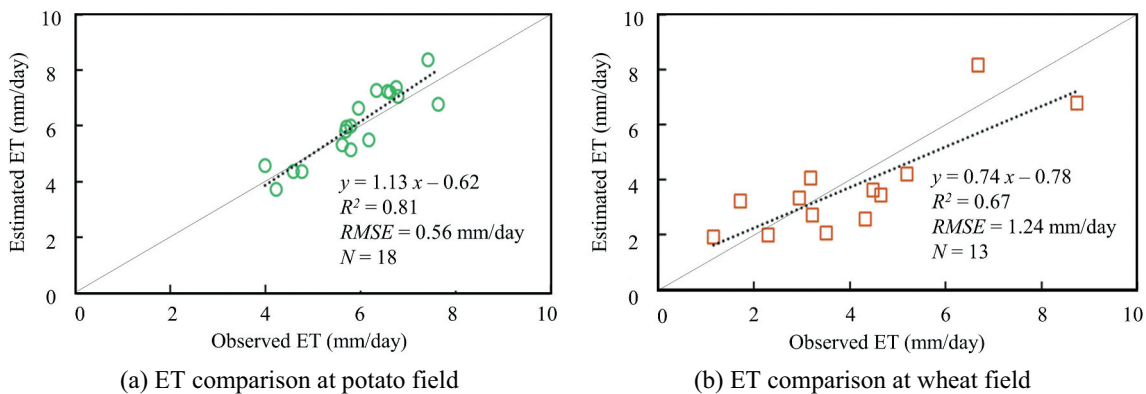(a) ET comparison at potato field

(b) ET comparison at wheat field

Figure 5. Comparison of ETMonitor estimated ET_a ($Ec+Es$) with in-situ measurements for potato (a) and wheat (b) during the non-irrigation days for the growing season in 2019.
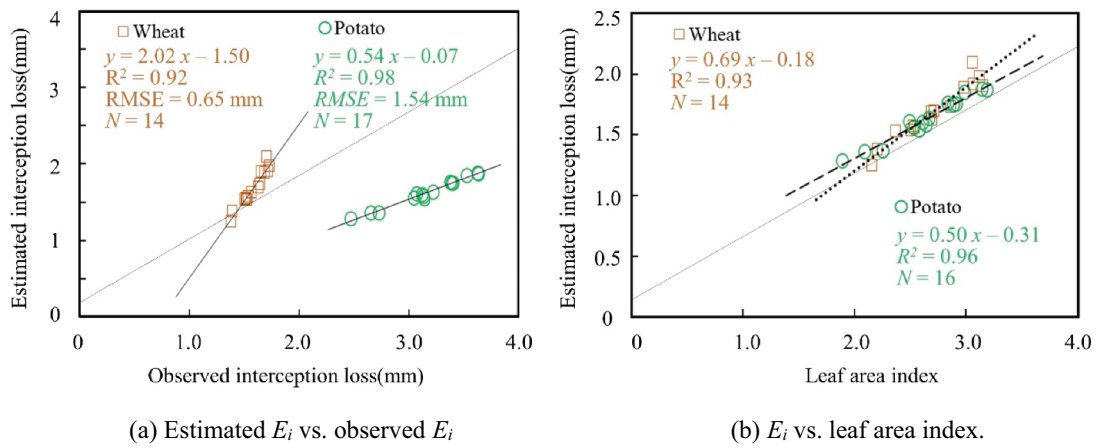
Figure 6. Comparison of estimated interception loss (E_i) with ground observed E_i (a) and with leaf area index (b) for wheat and potato during the irrigation days for growing season in 2019.

($RMSE$ = 0.64 mm) than for potato ($RMSE$ = 1.54 mm) (Figure 6). The estimated and measured E_i for wheat were rather close, probably due to an even distribution of the crop in the field, which makes it easier to perform accurate measurements of interception. In contrast, a significant difference was observed for potato, which could be due to several factors (Beinum and Beulke 2010), such as row cropping pattern, variable fractional vegetation cover, and the position of the instrument at the bottom of the canopy, which plays a major role in the reference measurements. There is an obvious and direct relationship between the FVC and the estimated E_i, as demonstrated by several studies (Cui and Jia 2014; Cui et al. 2017; Y. K. Cui et al. 2015; Zheng and Jia 2020; Zheng et al. 2016). The LAI is also an important canopy property that determines the water-holding capacity of a vegetation canopy. It

appears that E_i is related to LAI in the same way for the potato and wheat canopies (Figure 6).

This difference between the nozzle discharge and the water reaching the top of the canopy (as explained in section 3.2.3 and Figure 4) is further used to validate the estimates from our parameterization of droplet evaporation (Equation (5)). The DMT observations on two simultaneous days, including samples from all the six fields, were grouped into two separate dates (Figure 7), taking into account the difference in the local weather conditions between the 2 days. Two different trends were observed in the linear regression of the estimated E_A against the measurements on the two dates, 13th and 14th July of 2019, when plotted separately (Figure 7). This can be attributed to the difference in air temperature, vapor pressure deficit and wind speed. The correlation between the measured and estimated values was very high and very
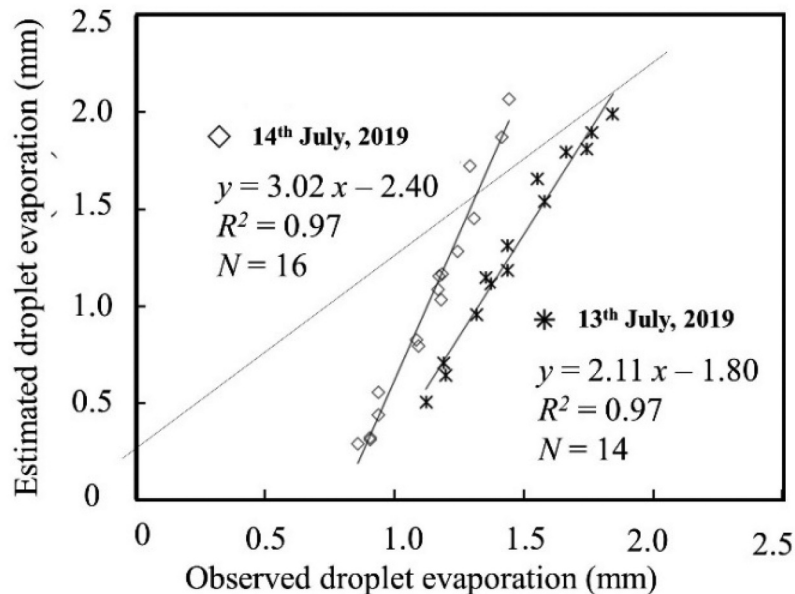

Figure 7. Comparison of measured and estimated water droplet evaporation (E_A) during sprinkling on 13th July and 14th July, 2019.

similar on both days, i.e. $R^2 = 0.97$, with a steeper variation 14th July than that on 13th July, 2019, which means that there was a greater variation in the estimated E_A compared to the reference measurements on 14th July than that on 13th July.

4.2. Variation of the irrigation consumptive water use

The *GIWU* components estimated with our parameterization illustrate the spatial variability very efficiently at 10 m spatial resolution (Figure 8). E_c ranges between 4 and 7 mm/day in each field, with higher values over wheat as wheat is in its peak growth stage on 14th July, 2019. On average E_s varies between 1.8 and 2.5 mm/day, with higher values over recently irrigated soil (using visual image interpretation technique), such as in a potato field (right middle field in Figure 8). Wet soils tend to have a lower albedo, which is very well captured by the E_s component of ETMonitor. E_i is between 0.5 and 2.5 mm per irrigation event for both crops. The estimated sprinkler droplet evaporation clarifies the difference in droplet evaporation between the center (0.2 mm/irrigation) and the outer lateral end (4 mm/irrigation) as a result of differences in operating pressure, larger air mass exposure and lateral tangential speed of the sprinkling system. Higher irrigation volume by sprinkler heads closer to the center (in wheat fields) is well reflected in the E_C, E_S, and E_i, thus reflecting accuracy at higher spatial resolution and efficient monitoring of the *GIWU*.

All the *GIWU* components were estimated at daily scale for potato and wheat (Figure 9). As expected, the maximum evapotranspiration ET_C was higher than actual evapotranspiration ET_a on most days for both potato and wheat. ETMonitor correctly estimated the partitioning into soil evaporation and canopy transpiration, e.g. during the early growth stage of potato (up to DOY-170) when the fractional soil cover was

greater than the vegetation, with E_s being consistently higher than E_c. Apart from the meteorological forcing, the variation in daily actual E_c and E_s is largely dependent on the surface properties used in ETMonitor (Hu and Jia 2015) to parameterize the energy and mass exchange at the land–atmosphere interface.

Regarding the variables directly related to the irrigation events, E_i is negligible (0 mm/day) in the early stage of crop growth, while it starts to increase in the development stage when FVC is more than 0.5 and the frequency of irrigation increases, reaching its maximum, i.e. 2.3 mm/day for potato and 2.1 mm/day for wheat, in the mid-season when the canopy cover is maximum for both crops. E_i accounts for 13.3% (potato) and 12.12% (wheat) of the water delivered by the sprinkler (17.3 mm) per irrigation.

E_A depends on the weather conditions and the operating pressure of the sprinkler nozzles and is well captured by our estimates. It is illustrated by the fact that E_A varies between 1 mm and 5 mm per irrigation in response to the weather conditions, which drive ET_a in a similar way. The loss due to E_A (2–5 mm) is rather constant across all irrigation events, regardless of the vegetation cover.

4.3. Variation of the irrigation water requirement

Figure 10 shows the maximum crop (unstressed) evapotranspiration (ET_C) for potato and wheat determined by Equation (8) in the whole growing season of 2019 in the study area. This maximum crop evapotranspiration of each crop can be used to estimate the *CWR* using Equation (7). The daily variation in ET_C due to local weather conditions (ET_0) and growth stage (k_c) is well reflected in both crops, where the ET_C for potato varies between 4 mm/day and 8 mm/day during the mid-growth stage. In the case of wheat, ET_C shows a narrower but higher range between 6 mm/day and 8.5 mm/day during the mid-growth stage. The early growth stage of wheat is characterized
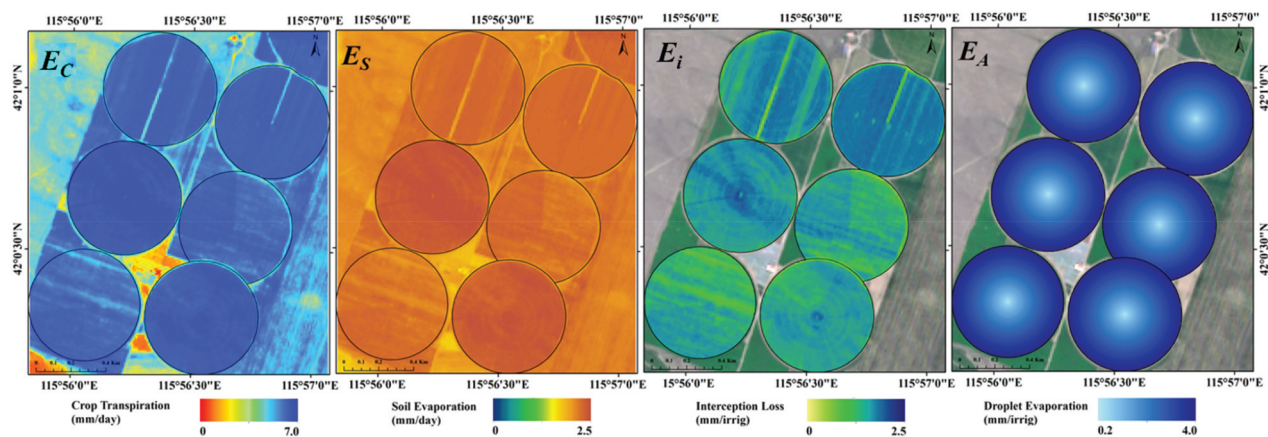

Figure 8. Spatial distribution of daily estimates of crop transpiration (E_c), soil evaporation (E_s), interception loss (E_i), and droplet evaporation (E_A) on 14th July of 2019 in the study area.
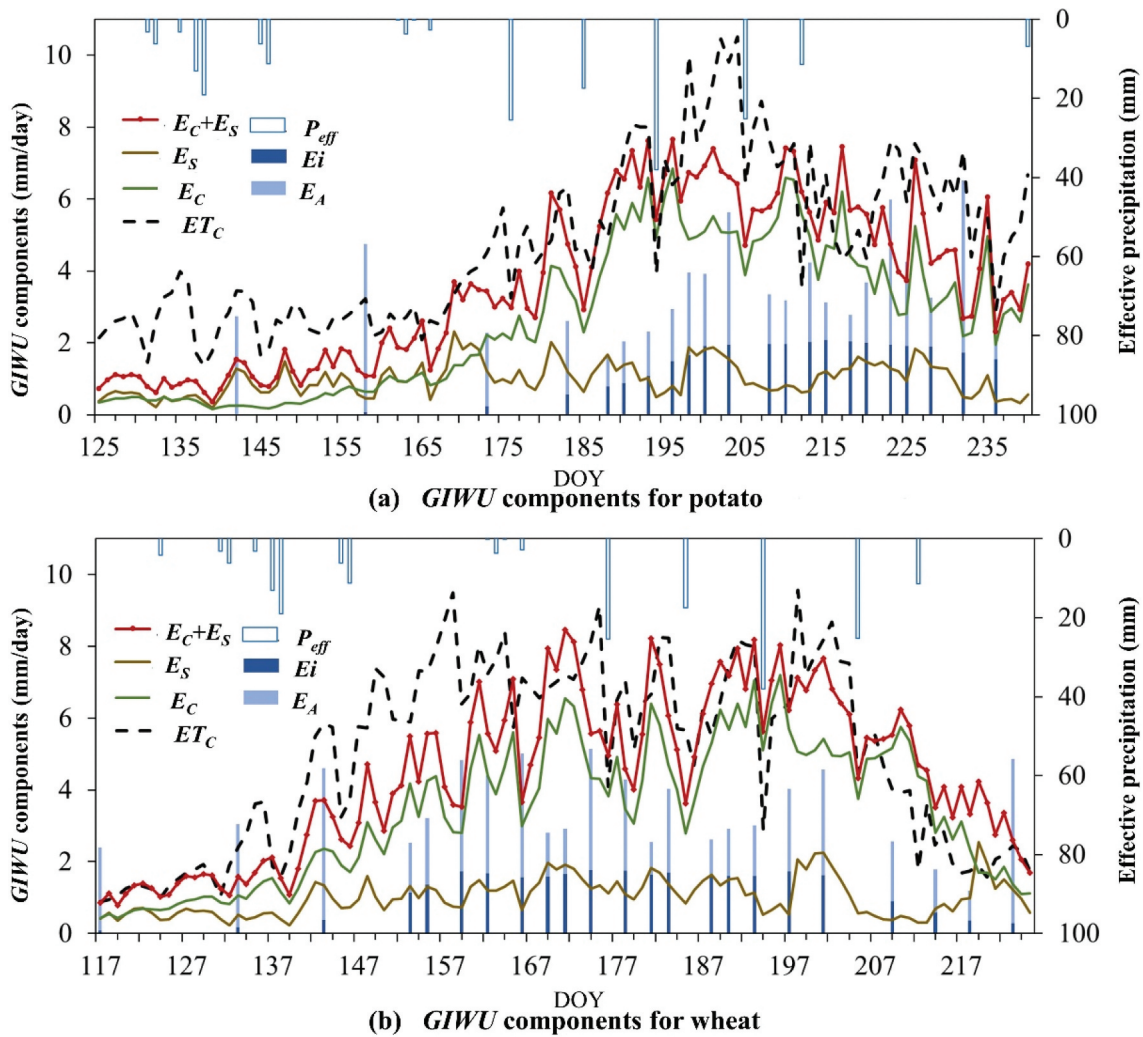
Figure 9. Daily variation of *GIWU* components for potato and wheat for the whole growing season in 2019.

by a shorter and steeper increase in the ET_C due to the denser planting of wheat (5 cm between rows) in contrast to potato, where potato plants are sparser, i.e. 90 cm between rows and 20 cm along rows. This results in a higher rate of vegetation cover change in wheat compared to potato.

During the early growth stage, k_c of both crops remained low, close to 0.2, and started to increase gradually during the development stage (Figure 10). During the canopy development, k_c varies between 0.3 and 1.2 for potato and 0.36 to 1.32 for wheat until the mid-growth stage with the highest canopy cover. The most contrasting is the late growth stage of both crops, resulting in a decrease in the k_c values (1.3 to 0.4) compared to potato (1.24 to 1.02) which is harvested within 5 days of maturity. The k_c-NDVI based crop coefficient has proven to be accurate in providing dense time series and can identify different crop phenological stages (Choudhury et al. 1994; Johnson and Trout 2012), unlike the generic k_c and number of days provided by FAO 56 (Allen et al. 1998) which can only provide a tabular form of k_c at specific phenological stages.

4.4. Irrigation performance evaluation

The ultimate objective of this study is achieved through the evaluation of *IPs*, which is based on an integrated estimation and understanding of the crop water requirements at field level and the amount of water actually used at different levels within an irrigation system (Table 5 and Figure 11). ETMonitor has efficiently quantified the transpiration and evaporation from crop and soil using high-resolution remote sensing data from Sentinel-2 MSI and Landsat-8 OLI Level-2 for the 2019 growing season. The estimated ET_a ($=E_c + E_s + E_i$) were 455.8 mm (potato) and 508 mm (wheat). These results are consistent with previous studies (Feng et al. 2023; Li et al. 2003), which showed the average ET of potato ranged from 250 mm/yr to 422 mm/yr in Northern China. The estimated ET of wheat was also comparable with the spring wheat (Li et al. 2023; Tong, Kang, and Zhang 2007), but higher than the winter wheat in the North China plain (Zhang et al. 2022), most likely due to the much higher atmosphere water demand of spring wheat during summer period in the study region. Droplet evaporation E_A was
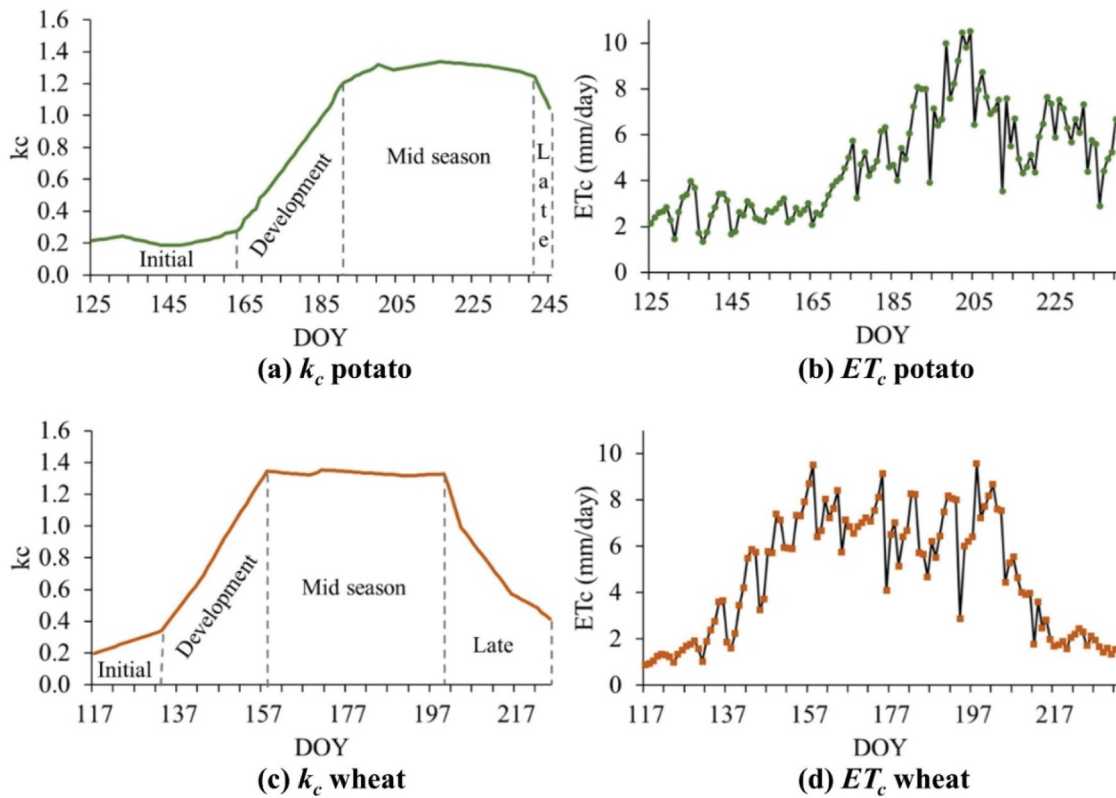
Figure 10. Daily k_c and ET_C for potato and wheat for the growing season in 2019 in the study area.

Table 5. Summary of the estimated components of water use and water requirement for the irrigation performance indicators of the growing season (27th April–4th October, 2019) in 2019 in the study area.

Components	Potato (mm)	Wheat (mm)
Crop Water Requirement (CWR) [ET_c]	555.0	538.2
Precipitation (P_{tot})	214.5	211.7
Effective precipitation (P_{eff})	140.9	140.0
Water Allocation (V)	306.2	334.3
Droplet evaporation (E_A)	46.1	50.8
Interception loss (E_i)	31.7	28.5
Plant transpiration and soil evaporation from ETMonitor [$E_c + E_s$]	424.1	479.5
Net Irrigation water requirement (NIWR) [$CWR - P_{eff}$]	414.1	398.2
Gross Irrigation water requirement (GIWR) [$NIWR + loss$]	534.4	513.8
Gross irrigation water use (GIWU) [$(ET_a - P_{eff}) + loss$]	361.0	418.8
Irrigation Performance (IP1) [NIWR/V]	**1.4**	**1.2**
Irrigation Performance (IP2) [GIWR/V]	**1.6**	**1.4**
Irrigation Performance (IP3) [GIWR/GIWU]	**1.4**	**1.1**

estimated as 46 mm and 51 mm and interception loss E_i as 32 mm and 28 mm for each crop during the whole growing season. These correspond to a total loss of 25.4% and 23.7% of the total water allocated to each crop, respectively. The GIWU by the CPIS was estimated to be 361 mm for potato and 419 mm for wheat for the whole growing season.

The CWR was estimated to be 555.0 mm for potato and 538.2 mm for wheat. The P_{eff} was estimated to be 140 mm, much lower than the CWR, resulting in the NIWR of 414.1 mm and 398.2 mm for potato and wheat, respectively. The GIWR in a standard CPIS would be 534.4 mm and 513.8 mm for optimal growth of potato and wheat, respectively. Irrigation was recognized as the most effective way of increasing crop yield, and farmers apply supplemental irrigation for two to four times by pumping groundwater for increasing crop yield and maximizing economic benefits (Li et al. 2023). According to the irrigation schedule (Table 5), the total water amount allocated to potato and wheat was estimated to be 306 mm and 334 mm, respectively. Comparably, the averaged net irrigation requirement rates of spring wheat was 353.20 mm in the Shiya river basin in the Northeast China with much drier climate (Kong et al. 2023). This large amount of irrigation from groundwater may result in serious environmental impacts such as soil salinization and groundwater depletion, which are threatening the sustainability of local agricultural production and water resource management (Shi et al. 2023).
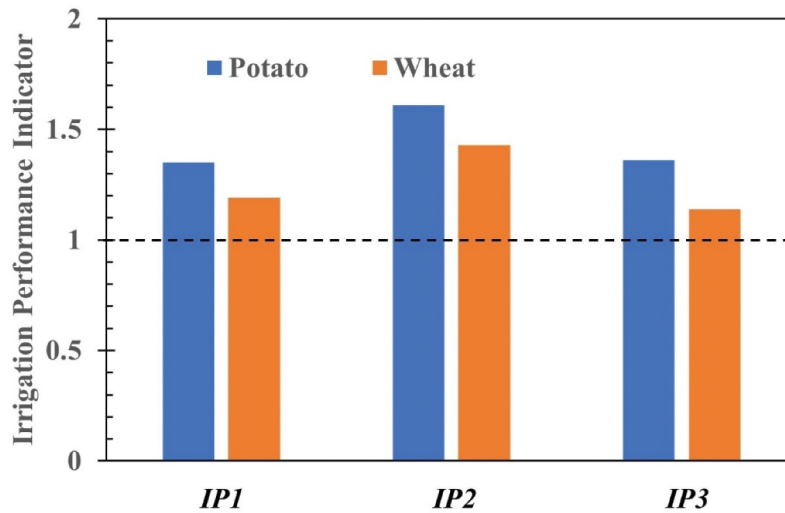
Figure 11. Graphical representation of different *IPs* of CPIS estimated in this study.

The *IP*-values show that in most cases the CPIS was underperformed. Water allocation was not even sufficient to meet *NIWR*, i.e. *IP1* = 1.35 for potato and 1.19 for wheat. The *IP2* values, i.e. 1.61 for potato and 1.43 for wheat, showed that the allocated water was insufficient to meet the crop water requirements estimated according to the FAO guidelines (Allen et al. 1998). The overall performance of the irrigation system was highly insufficient, *IP3* = 1.36 for potato and 1.14 for wheat. *IP2* and *IP3* can be considered as the best way to evaluate the performance of any irrigation system, which includes not only the *NIWR* (like in *IP1*) but also application losses. They take into account the actual practice of water application by the farmer/land-holder/administrative divisions and the standardized efficiency of the irrigation system (to achieve optimum requirement) to evaluate the actual water use.

It should also be noted that the *IPs* in this study focus on different aspects of water, e.g. water use and requirement, while they do not include crop yield, which is farmer's final product. Integrated performance indicators, e.g. crop water productivity (*CWP*, equal to the ratio of crop yield to crop water consumption), are helpful and suggested for further studies to provide a more comprehensive analysis. A higher *CWP* results in either the same crop yield from less water resources, or a higher yield from the same water resources, so *CWP* could be of direct benefit for farmers. A moderate deficit irrigation has been shown to lead to similar yields and increased *CWP* (Asmamaw et al. 2021; Fereres and Soriano 2007; Yang et al. 2022). Given the limited availability of water resources, technologies, and theories to improve the irrigation practice for higher CWP are highly appreciated for farmers and water management sectors.

5. Conclusions

This study contributes to evaluate the performance of an irrigation system toward precision irrigated agriculture, and it is achieved through the comprehensive evaluation of the irrigation water requirement and actual water use considering the water losses. This is achieved mainly by integrated usages of hydrological modeling and satellite remote sensing at high spatial and temporal resolution. The loss due to droplet evaporation directly from the air is fairly constant (2–5 mm) across all the irrigation events regardless of vegetation cover. The loss due to evaporation of canopy intercepted water remains negligible (0 mm) during the early stage of crop growth and reaches its maximum of 2.3 mm for potato and 2.1 mm for wheat per irrigation event during the mid-season when the canopy cover is maximum for both crops. This accounts for 13.3% (potato) and 12.12% (wheat) of the sprinkler discharge. The precise proportion of losses estimated during each application can be attributed to our proposed approach in mapping both components. The estimates of gross irrigation water use were in good agreement with the ground observations, with R^2 of 0.64–0.81 for actual water use and 0.66–0.97 for water losses. The *RMSE* was 0.59–1.82 mm/day for actual daily water use and 0.64–1.55 mm/day for water losses for each irrigation, respectively. The daily variation of each component of gross irrigation water requirement and gross irrigation water use reflects a good relationship between each other. Information on the actual practice of the farmer was collected and used to estimate the amount of irrigation to be applied only during the irrigation events. This is very helpful for the correct representation of the irrigation practice in the new approach proposed in this study. Overall, the study shows that center pivot irrigation system has underperformed in minimizing water losses with losses

of 52,897.5 m³/season, i.e. 25.4% of the total amount of water applied, for wheat and 103,807.2 m³/season, i.e. 23.7% for potato in the study area. Each of the *IPs* addresses a specific aspect of the efficiency of the irrigation system. This implies that the amount of water applied was largely insufficient to meet the gross water requirements, i.e. including losses. These imply the necessity to improve the irrigation practice to use the water more efficiently and save water given that the water resource is limited.

ETMonitor, driven by mainly high spatial resolution remote sensing data, can play a critical role in characterizing actual water use. The combined use of Sentinel-2 MSI Level-2 and Landsat-8 OLI Level-2 multi-spectral images provided data with higher temporal frequency to generate daily field-scale estimates of crop water requirements and use. A good accuracy was achieved in estimating evaporation. The same was applicable to identify the spatial uniformity of irrigation application, which was captured by the detailed maps of irrigation components using high-resolution satellite data and simulation models. It is highly recommended to consider the irrigation method and farmers' practice to estimate crop water requirement and consumptive water use by using satellite image data as well as to evaluate the performance of an irrigation system. The proposed method is helpful to evaluate the performance of irrigation water management systems, and it could be further improved by integrating with more comprehensive indicators (e.g. crop water productivity) to support agricultural water use efficiency evaluation.

Disclosure statement

Funding

Notes on contributors

Chaolei Zheng is an associate professor at the Aerospace Information Research Institute, Chinese Academy of Sciences, China. He received his Ph.D. degree from Shizuoka University in 2013. His research interests include the remote-sensing-based modeling and monitoring of evapotranspiration, soil moisture downscaling, global water resource products development and application.

Li Jia is a leading scientist in Earth observation for terrestrial water cycle, water resource and climate change at the Aerospace Information Research Institute, Chinese Academy of Sciences. She is currently a member of the WCRP GEWEX-SSG (Global Energy and Water Exchanges program Scientific Steering Group). She received the Ph.D. degree in environmental science from Wageningen University, Wageningen, The Netherlands, in 2004. Her research interests include the study of earth observation and its applications in hydrometeorology, water resource, agriculture, and climate change.

Massimo Menenti held senior research positions in The Netherlands, France, USA, China, and Italy. He is currently a foreign expert at the Aerospace Information Research Institute, Chinese Academy of Sciences, Beijing, China. His best-known achievements have been attained in the aspects of surface parameter retrievals from remote-sensing, remote-sensing-based evapotranspiration estimation, and the application of remote sensing technology in hydrology and climate models.

Guangcheng Hu received a Ph.D. degree in groundwater science and engineering from the China University of Geosciences, Beijing, China, in 2010. He is an assistant professor with the Aerospace Information Research Institute, Chinese Academy of Sciences. His research interest is the remote-sensing-based evapotranspiration estimation.

Jing Lu is an assistant professor at the Aerospace Information Research Institute, Chinese Academy of Sciences, China. She received her Ph.D. in Geographic Information System (GIS) in 2014 from the Institute of Geographic Sciences and Natural Resources Research, Chinese Academy of Science. Her research focuses on remote sensing-based evapotranspiration estimation, drought monitoring, and water resource evaluation.

Qiting Chen received a Ph.D. degree in Cartography and Geographic Information Systems from Aerospace Information Research Institute, Chinese Academy of Sciences, Beijing, China, in 2017. She is an Assistant Researcher with the Aerospace Information Research Institute, Chinese Academy of Sciences. Her research interests include the remote-sensing-based water use efficiency estimation and atmosphere-land surface interaction.

Min Jiang is an Assistant Professor at the Aerospace Information Research Institute, Chinese Academy of Sciences, China. He received his Ph.D. degree in physical geography from the University of Chinese Academy of Sciences, Beijing, China, in 2019. His research interests include terrestrial ecosystem water-use efficiency, vegetation change and drought monitoring, land use and cover change and its environmental effects.

Marco Mancini is a professor at Department of Civil and Environmental Engineering at Politecnico di Milano (Italy). His research activity focuses on hydrological processes and their interactions with anthropic activities for quantification of the design variables of engineering hydraulic works and water resource systems. He has developed and continuously upgrades research on distributed hydrological models driven by remote sensing data.

Chiara Corbari is Associate Professor at Department of Civil and Environmental Engineering at Politecnico di Milano (Italy). Her expertise is focused on the study of the

water and energy cycles, integrating land surface models with remote-sensing data and ground measurements for assessing continuous in time evapotranspiration and soil moisture estimates at detail spatial and temporal resolution over large agricultural areas as well as at fields scale.

ORCID

Chaolei Zheng http://orcid.org/0000-0002-6085-8274
Li Jia http://orcid.org/0000-0002-3108-8645
Massimo Menenti http://orcid.org/0000-0001-9176-4556
Guangcheng Hu http://orcid.org/0000-0003-2940-8336
Jing Lu http://orcid.org/0000-0003-2149-7071
Min Jiang http://orcid.org/0000-0002-3510-9829
Chiara Corbari http://orcid.org/0000-0002-1490-3847

Data availability statement

The data that support the findings of this study are available from the corresponding author on reasonable request.

References

Akdim, N., S. Alfieri, A. Habib, A. Choukri, E. Cheruiyot, K. Labbassi, and M. Menenti. 2014. "Monitoring of Irrigation Schemes by Remote Sensing: Phenology versus Retrieval of Biophysical Variables." *Remote Sensing* 6 (6): 5815–5851. https://doi.org/10.3390/rs6065815.

Allen, R. G., L. S. Pereira, D. Raes, and M. Smith. 1998. "Crop Evapotranspiration—Guidelines for Computing Crop Water Requirements; FAO Irrigation and Drainage Paper 56." FAO: Rome, Italy, p. 300. 17. https://doi.org/10.1016/j.eja.2010.12.001.

Asmamaw, D. K., P. Janssens, M. Desse, S. Tilahun, E. Adgo, J. Nyssen, K. Walraevens, and W. Cornelis. 2021. "Deficit Irrigation as a Sustainable Option for Improving Water Productivity in Sub-Saharan Africa: The Case of Ethiopia a Critical Review." *Environmental Research Communications* 3 (10): 102001. https://doi.org/10.1088/2515-7620/ac2a74.

Bastiaanssen, W. G. M., and M. G. Bos. 1999. "Irrigation Performance Indicators based on Remotely Sensed Data: A Review of Literature." *Irrigation and Drainage Systems* 13 (4): 291–311. https://doi.org/10.1023/A:1006355315251.

Beinum, W. V., and S. Beulke. 2010. "Collection and Evaluation of Relevant Information on Crop Interception for the Revision of the Guidance Document on Persistence in Soil." *EFSA Supporting Publications* 9 (10): 41. https://doi.org/10.2903/sp.efsa.2010.EN-73.

Bennour, A., L. Jia, M. Menenti, C. Zheng, Y. Zeng, B. A. Barnieh, and M. Jiang. 2022. "Calibration and Validation of SWAT Model by Using Hydrological Remote Sensing Observables in the Lake Chad Basin." *Remote Sensing* 14 (6): 1511. https://doi.org/10.3390/rs14061511.

Buri, P., S. Fatichi, T. E. Shaw, C. L. Fyffe, E. S. Miles, M. J. McCarthy, M. Kneib, et al. 2024. "Land Surface Modeling Informed by Earth Observation Data: Toward Understanding Blue–Green–White Water Fluxes in High Mountain Asia." *Geo-Spatial Information Science* 1–25. https://doi.org/10.1080/10095020.2024.2330546.

Bwambale, E., Z. Naangmenyele, P. Iradukunda, K. M. Agboka, E. A. Houessou-Dossou, D. A. Akansake,

M. E. Bisa, et al. 2022. "Towards Precision Irrigation Managemen T: A Review of GIS, Remote Sensing and Emerging Technologies." *Cogent Engineering* 9 (1): 2100573. https://doi.org/10.1080/23311916.2022.2100573.

Calera, A., I. Campos, A. Osann, G. D'Urso, and M. Menenti. 2017. "Remote Sensing for Crop Water Management: From ET Modelling to Services for the End Users." *Sensors (Switzerland)* 17 (5): 1–25. https://doi.org/10.3390/s17051104.

Carpenter, S. R., E. H. Stanley, and M. J. Vander Zanden. 2011. "State of the world's Freshwater Ecosystems: Physical, Chemical, and Biological Changes." *Annual Review of Environment and Resources* 36:75–99. https://doi.org/10.1146/annurev-environ-021810-094524. 1

Chen, Q., L. Jia, M. Menenti, R. Hutjes, G. Hu, C. Zheng, and K. Wang. 2019. "A Numerical Analysis of Aggregation Error in Evapotranspiration Estimates Due to Heterogeneity of Soil Moisture and Leaf Area Index." *Agriculture and Forest Meteorology* 269-270:335–350. https://doi.org/10.1016/j.agrformet.2019.02.017.

Chen, Q., L. Jia, M. Menenti, G. Hu, K. Wang, Z. Yi, J. Zhou, et al. 2023. "A Data-Driven High Spatial Resolution Model of Biomass Accumulation and Crop Yield: Application to a Fragmented Desert-Oasis Agroecosystem." *Ecological Modelling* 475:110182. https://doi.org/10.1016/j.ecolmodel.2022.110182.

Chen, N., X. Li, H. Shi, Y. Zhang, Q. Hu, and Y. Sun. 2023. "Modeling Effects of Biodegradable Film Mulching on Evapotranspiration and Crop Yields in Inner Mongolia." *Agricultural Water Management* 275:107996. https://doi.org/10.1016/j.agwat.2022.107996.

Choudhury, B. J., N. U. Ahmed, S. B. Idso, R. J. Reginato, and C. S. T. Daughtry. 1994. "Relations Between Evaporation Coefficients and Vegetation Indices Studied by Model Simulations." *Remote Sensing of Environment* 50 (1): 1–17. https://doi.org/10.1016/0034-4257(94)90090-6.

Chu, H., X. Luo, Z. Ouyang, W. S. Chan, S. Dengel, S. C. Biraud, M. S. Torn, et al. 2021. "Representativeness of Eddy-Covariance Flux Footprints for Areas Surrounding AmeriFlux Sites." *Agricultural and Forest Meteorology* 301–302:108350. https://doi.org/10.1016/j.agrformet.2021.108350.

Corbari, C., R. Salerno, A. Ceppi, V. Telesca, and M. Mancini. 2019. "Smart Irrigation Forecast Using Satellite LANDSAT Data and Meteo-Hydrological Modelling." *Agricultural Water Management* 212:283–294. https://doi.org/10.1016/j.agwat.2018.09.005.

Cui, Y., and L. Jia. 2014. "A Modified Gash Model for Estimating Rainfall Interception Loss of Forest Using Remote Sensing Observations at Regional Scale." *Water (Switzerland)* 6 (4): 993–1012. https://doi.org/10.3390/w6040993.

Cui, Y. K., L. Jia, G. C. Hu, and J. Zhou. 2015. "Mapping of Interception Loss of Vegetation in the Heihe River Basin of China Using Remote Sensing Observations." *IEEE Geoscience and Remote Sensing Letters* 12 (1): 23–27. https://doi.org/10.1109/LGRS.2014.2324635.

Cui, Y., P. Zhao, B. Yan, H. Xie, P. Yu, W. Wan, W. Fan, and Y. Hong. 2017. "Developing the Remote Sensing-Gash Analytical Model for Estimating Vegetation Rainfall Interception at Very High Resolution: A Case Study in the Heihe River Basin." *Remote Sensing* 9 (7): 661. https://doi.org/10.3390/rs9070661.

Dari, J., L. Brocca, S. Modanesi, C. Massari, A. Tarpanelli, S. Barbetta, R. Quast, et al. 2023. "Regional Data Sets of High-Resolution (1 and 6 Km) Irrigation Estimates from

Space." *Earth System Science Data* 15 (4): 1555–1575. https://doi.org/10.5194/essd-15-1555-2023.

D'Urso, G. 2010. "Current Status and Perspectives for the Estimation of Crop Water Requirements from Earth Observation." *Italian Journal of Agronomy* 5 (2): 107–120. https://doi.org/10.4081/ija.2010.107.

Du, D., C. Zheng, L. Jia, Q. Chen, M. Jiang, and G. Hu. 2022. "Estimation of Cropland Gross Primary Productivity by Integrating Water Availability Factor in Light-Use-Efficiency-Based Model and Satellite Observations." *Remote Sensing* 14 (7): 1722. https://doi.org/10.3390/rs14071722.

Evans, R. G., and E. J. Sadler. 2008. "Methods and Technologies to Improve Efficiency of Water Use." *Water Resources Research* 44 (7): W00E04. https://doi.org/10.1029/2007WR006200.

Feng, X., H. Liu, D. Feng, X. Tang, L. Li, J. Chang, J. Tanny, and R. Liu. 2023. "Quantifying Winter Wheat Evapotranspiration and Crop Coefficients Under Sprinkler Irrigation Using Eddy Covariance Technology in the North China Plain." *Agricultural water management* 277:108131. https://doi.org/10.1016/j.agwat.2022.108131.

Fereres, E., and M. A. Soriano. 2007. "Deficit Irrigation for Reducing Agricultural Water Use." *Journal of Experimental Botany* 58 (2): 147–159. https://doi.org/10.1093/jxb/erl165.

Gash, J. H. C., C. R. Lloyd, and G. Lachaud. 1995. "Estimating Sparse Forest Rainfall Interception with an Analytical Model." *Journal of Hydrology* 170 (1): 79–86. https://doi.org/10.1016/0022-1694(95)02697-N.

Gray, D., and D. Norum. 1967. "The Effect of Soil Moisture on Infiltration as Related to Runoff and Recharge." *Proceedings of Hydrology Symposium* 6:133–153. https://doi.org/10.1016/j.bbrc.2008.12.060.

Herbst, M., P. T. W. Rosier, D. D. McNeil, R. J. Harding, and D. J. Gowing. 2008. "Seasonal Variability of Interception Evaporation from the Canopy of a Mixed Deciduous Forest." *Agricultural and Forest Meteorology* 148 (11): 1655–1667. https://doi.org/10.1016/j.agrformet.2008.05.011.

Hu, G., and L. Jia. 2015. "Monitoring of Evapotranspiration in a Semi-Arid Inland River Basin by Combining Microwave and Optical Remote Sensing Observations." *Remote Sensing* 7 (3): 3056–3087. https://doi.org/10.3390/rs70303056.

Jarvis, P. G. 1976. "The Interpretation of the Variations in Leaf Water Potential and Stomatal Conductance Found in Canopies in the Field." *Philosophical Transactions of the Royal Society of London B: Biological Sciences* 273 (927): 593–610. https://doi.org/10.1098/rstb.1976.0035.

Jia, L., G. C. Hu, Q. T. Chen, and C. Zheng. 2021. "Crop Water Productivity Assessment of a Representative Irrigation District in Morocco." In Big Earth Data in Support of the Sustainable Development Goals (2020): The Belt and Road, edited by H. D. Guo, 67–73. Beijing: Science Press.

Jia, L., C. Zheng, G. Hu, and M. Menenti. 2018. "Evapotranspiration." In *Comprehensive Remote Sensing*, edited by S. Liang, 25–50. Oxford: Elsevier. https://doi.org/10.1016/B978-0-12-409548-9.10353-7.

Johnson, L. F., and T. J. Trout. 2012. "Satellite NDVI Assisted Monitoring of Vegetable Crop Evapotranspiration in California's San Joaquin Valley." *Remote Sensing* 4 (2): 439–455. https://doi.org/10.3390/rs4020439.

Kljun, N., P. Calanca, M. W. Rotach, and H. P. Schmid. 2015. "A Simple Two-Dimensional Parameterisation for Flux Footprint Prediction (FFP)." *Geoscientific Model Development* 8 (11): 3695–3713. https://doi.org/10.5194/gmd-8-3695-2015.

Knipper, K. R., W. P. Kustas, M. C. Anderson, J. G. Alfieri, J. H. Prueger, C. R. Hain, F. Gao, et al. 2019. "Evapotranspiration Estimates Derived Using Thermal-Based Satellite Remote Sensing and Data Fusion for Irrigation Management in California Vineyards." *Irrigation Science* 37 (3): 431–449. https://doi.org/10.1007/s00271-018-0591-y.

Kong, M., G. Wang, T. Guan, Y. Wu, and G. Liu. 2023. "Assessment of Net Irrigation Requirements for Spring Wheat and Spring Maize in Shiyanghe Watershed, Northwestern China." *Water Conservation Science and Engineering* 8 (1): 54. https://doi.org/10.1007/s41101-023-00228-6.

Kuo, S., S. Ho, and C. Liu. 2006. "Estimation Irrigation Water Requirements with Derived Crop Coefficients for Upland and Paddy Crops in ChiaNan Irrigation Association, Taiwan." *Agricultural Water Management* 82 (6): 433–451. https://doi.org/10.1016/j.agwat.2005.08.002.

Lankford, B. A. 2023. "Resolving the Paradoxes of Irrigation Efficiency: Irrigated Systems Accounting Analyses Depletion-Based Water Conservation for Reallocation." *Agricultural Water Management* 287:108437. https://doi.org/10.1016/j.agwat.2023.108437.

Levidow, L., D. Zaccaria, R. Maia, E. Vivas, M. Todorovic, and A. Scardigno. 2014. "Improving Water-Efficient Irrigation: Prospects and Difficulties of Innovative Practices." *Agricultural Water Management* 146:84–94. https://doi.org/10.1016/j.agwat.2014.07.012.

Liang, S., C. Shuey, H. Fang, C. Walthall, C. Daughtry, and R. Hunt. 2003. "Narrowband to Broadband Conversions of Land Surface Albedo: II. Validation." *Remote Sensing of the Environment* 84 (1): 25–41. https://doi.org/10.1016/S0034-4257(02)00068-8.

Li, Y., J. Cui, T. Zhang, and H. Zhao. 2003. "Measurement of Evapotranspiration of Irrigated Spring Wheat and Maize in a Semi-Arid Region of North China." *Agricultural Water Management* 61 (1): 1–12. https://doi.org/10.1016/S0378-3774(02)00177-4.

Lin, M., S. M. M. Sadeghi, and J. T. Van Stan. 2020. "Partitioning of Rainfall and Sprinkler-Irrigation by Crop Canopies: A Global Review and Evaluation of Available Research." *Hydrology* 7 (4): 76. https://doi.org/10.3390/hydrology7040076.

Liu, K., Y. Bo, X. Li, S. Wang, and G. Zhou. 2024. "Uncovering Current and Future Variations of Irrigation Water Use Across China Using Machine Learning." *Earth's Future* 12 (3): e2023EF003562. https://doi.org/10.1029/2023EF003562.

Liu, Y., Q. Zhuang, M. Chen, Z. Pan, N. Tchebakova, A. Sokolov, D. Kicklighter, et al. 2013. "Response of Evapotranspiration and Water Availability to Changing Climate and Land Cover on the Mongolian Plateau During the 21st Century." *Global and Planetary Change* 108:85–99. https://doi.org/10.1016/j.gloplacha.2013.06.008.

Li, Y., J. Wang, Q. Fang, Q. Hu, M. Huang, R. Chen, J. Zhang, B. Huang, Z. Pan, and X. Pan. 2023. "Optimizing Water Management Practice to Increase Potato Yield and Water Use Efficiency in North China." *Journal of Integrative Agriculture* 22 (10): 3182–3192. https://doi.org/10.1016/j.jia.2023.04.027.

Lloyd, C. R., J. H. C. Gash, W. J. Shuttleworth, and A. D. Marques. 1988. "The Measurement and Modeling of Rainfall Interception by Amazonian Rain Forest." *Agricultural and Forest Meteorology* 43 (3–4): 277–294. https://doi.org/10.1016/0168-1923(88)90055-X.

Mandanici, E., and G. Bitelli. 2016. "Preliminary Comparison of Sentinel-2 and Landsat-8 Imagery for a Combined Use." *Remote Sensing* 8 (12): 1014. https://doi.org/10.3390/rs8121014.

Martin, D. L., D. C. Kincaid, and W. M. Lyle. 2007. "Chapter 16-Design and Operation of Sprinkler Systems." In *Design and Operation of Farm Irrigation Systems*, edited by G. Hoffman, R. G. Evans, M. E. Jensen, D. L. Martin, and R. L. Elliott, 557–631. *2nd*. Michigan:American Society of Agricultural and Biological Engineers. https://doi.org/10.13031/2013.23699.

Menenti, M. 2000. "Irrigation and Drainage." *Journal of the Franklin Institute* 96 (5): 298–300. https://doi.org/10.1016/S0016-0032(73)90636-4.

Menenti, M., X. Li, L. Jia, K. Yang, F. Pellicciotti, M. Mancini, J. Shi, et al. 2021. "Multi-Source Hydrological Data Products to Monitor High Asian River Basins and Regional Water Security." *Remote Sensing* 13 (24): 5122–5129. https://doi.org/10.3390/rs13245122.

Menenti, M., T. N. M. Visser, J. A. Morabito, and A. Drovandi. 1989. "Appraisal of Irrigation Performance with Satellite Data and Georeferenced Information." In *Irrigation Theory and Practice. Inst. of Irrigation Studies*, edited by J. R. Rydzewski and C. F. Ward, 785–801. Southampton Univ. UK: Pentech Press.

Molle, B., S. Tomas, M. Hendawi, and J. Granier. 2012. "Evaporation and Wind Drift Losses During Sprinkler Irrigation Influenced by Droplet Size Distribution." *Irrigation and Drainage* 61 (2): 240–250. https://doi.org/10.1002/ird.648.

Pani, P., L. Jia, M. Menenti, G. Hu, C. Zheng, Q. Chen, and Y. Zeng. 2020. "Evaluating Crop Water Requirements and Actual Crop Water Use with Center Pivot Irrigation System in Inner Mongolia of China." *EGU General Assembly Conference Abstracts 2020*. https://doi.org/10.5194/egusphere-egu2020-12539.

Penman, H. L. 1948. "Natural Evapotranspiration from Open Water, Bare Soil and Grass." *Proceedings Royal Society of London, Series A* 193:120–146. https://doi.org/10.1098/rspa.1948.0037.

Playán, E., R. Salvador, J. M. Faci, N. Zapata, A. Martínez-Cob, and I. Sánchez. 2005. "Day and Night Wind Drift and Evaporation Losses in Sprinkler Solid-Sets and Moving Laterals." *Agricultural Water Management* 76 (3): 139–159. https://doi.org/10.1016/j.agwat.2005.01.015.

Reichle, R., G. De Lannoy, R. D. Koster, W. T. Crow, J. S. Kimball, and Q. Liu. 2018. "SMAP L4 Global 3-Hourly 9 Km EASE-Grid Surface and Root Zone Soil Moisture Geophysical Data, Version 4." In *Boulder, Colorado USA*: NASA National Snow and Ice Data Center Distributed Active Archive Center. https://doi.org/10.5067/KPJNN2GI1DQR.

Renault, D. 1999. "Offtake Sensitivity: Operation Effectiveness and Performance of Irrigation System." *Journal of Irrigation & Drainage Engineering* 125 (3): 137–147. https://doi.org/10.1061/(ASCE)0733-9437(1999)125:3(137).

Rivett, M. O., M. O. Cuthbert, R. Gamble, L. E. Connon, A. Pearson, M. G. Shepley, and J. Davis. 2016. "Highway Deicing Salt Dynamic Runoff to Surface Water and Subsequent Infiltration to Groundwater During Severe UK Winters." *Science of the Total Environment* 565:324–338. https://doi.org/10.1016/j.scitotenv.2016.04.095.

Roy, D. P., M. A. Wulder, T. R. Loveland, C. E. Woodcock, R. G. Allen, M. C. Anderson, and D. Helder. 2014. "Landsat-8: Science and Product Vision for Terrestrial Global Change Research." *Remote Sensing of Environment* 145:154–172. https://doi.org/10.1016/j.rse.2014.02.001.

Sayari, S., A. Mahdavi-Meymand, and M. Zounemat-Kermani. 2021. "Irrigation Water Infiltration Modeling Using Machine Learning." *Computers and Electronics in Agriculture* 180:105921. https://doi.org/10.1016/j.compag.2020.105921.

Schläpfer, D., C. C. Borel, J. Keller, and K. I. Itten. 1998. "Atmospheric Precorrected Differential Absorption Technique to Retrieve Columnar Water Vapour." *Remote Sensing of Environment* 65 (3): 353–366. https://doi.org/10.1016/S0034-4257(98)00044-3.

Shi, H., G. Luo, E. H. Sutanudjaja, O. Hellwich, X. Chen, J. Ding, S. Wu, et al. 2023. "Recent Impacts of Water Management on Dryland's Salinization and Degradation Neutralization." *Science Bulletin* 68 (24): 3240–3251. https://doi.org/10.1016/J.SCIB.2023.11.012.

Shuttleworth, W. J., and J. S. Wallace. 1985. "Evaporation from Sparse Crops—An Energy Combination Theory." *Quarterly Journal of the Royal Meteorological Society* 111 (469): 839–855. https://doi.org/10.1002/qj.49711146910.

Srivastava, P. K., P. C. Pandey, G. P. Petropoulos, N. N. Kourgialas, V. Pandey, and U. Singh. 2019. "GIS and Remote Sensing Aided Information for Soil Moisture Estimation: A Comparative Study of Interpolation Techniques." *Resources* 8 (2): 70. https://doi.org/10.3390/resources8020070.

Stambouli, T., A. Martínez-Cob, J. M. Faci, T. Howell, and N. Zapata. 2013. "Sprinkler Evaporation Losses in Alfalfa During Solid-Set Sprinkler Irrigation in Semiarid Areas." *Irrigation Science* 31 (5): 1075–1089. https://doi.org/10.1007/s00271-012-0389-2.

Steward, J. B. 1988. "Modelling Surface Conductance of Pine Forest." *Agricultural and Forest Meteorology* 43 (1): 19–35. https://doi.org/10.1016/0168-1923(88)90003-2.

Tariq, A., J. Yan, A. S. Gagnon, M. R. Khan, and R. Mumtaz. 2023. "Mapping of Cropland, Cropping Patterns and Crop Types by Combining Optical Remote Sensing Images with Decision Tree Classifier and Random Forest." *Geo-Spatial Information Science* 26 (3): 302–320. https://doi.org/10.1080/10095020.2022.2100287.

Thompson, A. L., J. R. Gilley, and J. M. Norman. 1993. "A Sprinkler Water Droplet Evaporation and Plant Canopy Model: II. Model Application." *Transactions - American Society of Agricultural Engineers: General Edition* 36 (3): 743–750. https://doi.org/10.13031/2013.28393.

Tolk, J. A., T. A. Howell, J. L. Steiner, D. R. Krieg, and A. D. Schneider. 1995. "Role of Transpiration Suppression by Evaporation of Intercepted Water in Improving Irrigation Efficiency." *Irrigation Science* 16 (2): 89–95. https://doi.org/10.1007/BF00189165.

Tong, L., S. Kang, and L. Zhang. 2007. "Temporal and Spatial Variations of Evapotranspiration for Spring Wheat in the Shiyang River Basin in Northwest China."

Agricultural Water Management 87 (3): 241–250. https://doi.org/10.1016/j.agwat.2006.07.013.

Uddin, M. J., and S. R. Murphy. 2020. "Evaporation Losses and Evapotranspiration Dynamics in Overhead Sprinkler Irrigation." *Journal of Irrigation & Drainage Engineering* 146 (8): 04020023. https://doi.org/10.1061/(asce)ir.1943-4774.0001469.

van Dijk, A. I. J. M., J. H. Gash, E. van Gorsel, P. D. Blanken, A. Cescatti, C. Emmel, B. Gielen, et al. 2015. "Rainfall Interception and the Coupled Surface Water and Energy Balance." *Agricultural and Forest Meteorology* 214–215:402–415. https://doi.org/10.1016/j.agrformet.2015.09.006.

Vermote, E. F., and S. Kotchenova. 2008. "Atmospheric Correction for the Monitoring of Land Surfaces." *Journal of Geophysical Research: Atmospheres* 113 (D23). https://doi.org/10.1029/2007JD009662.

Yang, B., P. Fu, J. Lu, F. Ma, X. Sun, and Y. Fang. 2022. "Regulated Deficit Irrigation: An Effective Way to Solve the Shortage of Agricultural Water for Horticulture." *Stress Biology* 2:28. https://doi.org/10.1007/s44154-022-00050-5.

Yazar, A. 1984. "Evaporation and Drift Losses from Sprinkler Irrigation Systems Under Various Operating Conditions." *Agricultural Water Management* 8 (4): 439–449. https://doi.org/10.1016/0378-3774(84)90070-2.

Zhang, Y., X. Guo, H. Pei, L. Min, F. Liu, and Y. Shen. 2022. "Evapotranspiration and Carbon Exchange of the Main Agroecosystems and Their Responses to Agricultural Land Use Change in North China Plain." *Agriculture, Ecosystems and Environment* 338:108103. https://doi.org/10.1016/j.agee.2022.108103.

Zheng, C., G. Hu, Q. Chen, and L. Jia. 2021. "Impact of Remote Sensing Soil Moisture on the Evapotranspiration Estimation." *National Remote Sensing Bulletin* 25 (4): 990–999. https://doi.org/10.11834/jrs.20210038 . in Chinese with English abstract.

Zheng, C., and L. Jia. 2020. "Global Canopy Rainfall Interception Loss Derived from Satellite Earth Observations." *Ecohydrology* 13 (2): e2186. https://doi.org/10.1002/eco.2186.

Zheng, C., L. Jia, and G. Hu. 2022. "Global Land Surface Evapotranspiration Monitoring by ETMonitor Model Driven by Multi-Source Satellite Earth Observations." *Journal of Hydrology* 613:128444. https://doi.org/10.1016/j.jhydrol.2022.128444.

Zheng, C., L. Jia, G. Hu, and J. Lu. 2019. "Earth Observations-Based Evapotranspiration in Northeastern Thailand." *Remote Sensing* 11 (2): 138. https://doi.org/10.3390/rs11020138.

Zheng, C., L. Jia, G. Hu, J. Lu, K. Wang, and Z. Li. 2016. "Global Evapotranspiration Derived by ETMonitor Model Based on Earth Observations." Paper Presented at *The International Geoscience and Remote Sensing Symposium* Beijing, China, July 11–15, 222–225.https://doi.org/10.1109/IGARSS.2016.7729049.

Zhou, J., L. Jia, M. Menenti, and B. Gorte. 2016. "On the Performance of Remote Sensing Time Series Reconstruction Methods – A Spatial Comparison." *Remote Sensing of Environment* 187:367–384. https://doi.org/10.1016/j.rse.2016.10.025.